Signal Processing 92 (2012) 1032–1043

Contents lists available at SciVerse ScienceDirect

Signal Processing

journal homepage: www.elsevier.com/locate/sigpro

DOA estimation of wideband sources without estimating the number of sources

Vinod V. Reddy*, B.P. Ng, Ying Zhang, Andy W.H. Khong

School of Electrical and Electronic Engineering, Nanyang Technological University, Nanyang Avenue, Singapore 639798, Singapore

ARTICLE INFO

Article history:
Received 27 April 2011
Received in revised form
17 October 2011
Accepted 19 October 2011
Available online 28 October 2011

Keywords:
Wideband DOA estimation

ABSTRACT

In this paper, we propose a new technique to estimate wideband source directions from the sensor snapshots without requiring to know the number of sources present in the scenario. This work is motivated by the fact that the existing model order estimation (number of sources) techniques for wideband source scenario are either inaccurate or computationally expensive. Direction-of-arrival (DOA) estimation is realized using a beamformer framework which imposes nulls in the spatial spectrum along the source directions. The null width along the frequency axis is widened by introducing a new data dependent term into the optimization problem, thus achieving wideband capability. Furthermore, the temporal processing of the data snapshots drastically reduces the number of snapshots required for wideband DOA estimation. The effectiveness of the proposed formulation is studied with simulated experiments.

© 2011 Elsevier B.V. All rights reserved.

1. Introduction

The two advanced and most explored problems in array processing are direction of arrival (DOA) estimation and beamforming [1]. The solution to these two problems is incorporated in many applications such as SONAR, RADAR and wireless communications among others. The problem is more challenging when the sources are wideband in nature. While the narrowband DOA estimation is advancing towards increasing the degrees-of-freedom using virtual array concept [2,3], wideband DOA estimation techniques have been proposed with some degree of success in coherent signal processing and improvements in DOA resolution. However, unlike narrowband DOA estimation, they have yet to achieve super-resolution capabilities for arbitrary array geometries.

For wideband DOA estimation, the signal model widely used to process data is given by

$$\mathbf{x}(f,l)=\mathbf{A}(f,\Theta)\mathbf{s}(f,l)+\mathbf{v}(f,l), \tag{1}$$

where $\mathbf{x}(f,l),\mathbf{v}(f,l)\in\mathbf{C}^{L\times 1}$ are the sensor snapshot vector and the additive noise vector in the frequency–time frame index $(f,\ l)$, respectively with L being the array size. The $M\times 1$ signal vector $\mathbf{s}(f,l)$ is multiplied with $\mathbf{A}(f,\Theta)\in\mathbf{C}^{L\times M}$ whose columns are the steering vectors corresponding to all the source directions Θ at frequency f.

Incoherent techniques, such as that proposed in [4], estimates source directions from the spectrum obtained by the superposition of narrowband MUSIC spectra evaluated across several frequency bins independently. The power variations in different frequency bins adversely affect the DOA estimates. Moreover, such techniques cease to distinguish coherent sources present in the scenario. Alternatively, data from several frequency bins are coherently unified in [5–7] to estimate source directions. The Coherent Signal Subspace Method (CSSM) [5] first transforms the data correlation matrices from all the subbands to a single focussing frequency. Narrowband DOA estimation is performed on a single correlation matrix obtained by averaging

* Correspondence to:. School of EEE, Block S2, Information Systems Research Laboratory, #B3a-06 Nanyang Avenue, Singapore 639798, Singapore. Tel.: +65 91980034.

E-mail addresses: vinodreddy@pmail.ntu.edu.sg (V.V. Reddy), ebpng@ntu.edu.sg (B.P. Ng), ZH0045NG@ntu.edu.sg (Y. Zhang), AndyKhong@ntu.edu.sg (A.W.H. Khong).

0165-1684/$ - see front matter © 2011 Elsevier B.V. All rights reserved.
doi:10.1016/j.sigpro.2011.10.015

all the transformed matrices. Due to the inherent frequency smoothing, this technique can be employed for coherent source scenarios as well. The design of the transformation matrices, popularly known as the *focussing matrices*, has drawn significant research interest [8–10]. The major limitation of CSSM however is the necessity for approximate initial DOA estimates to design the focussing matrices and the method's sensitivity to the initial estimates [11].

A recent noncoherent signal subspace technique known as the Test for Orthogonality of Projection Subspaces (TOPS) [12] has gained much interest since it does not require initial source direction estimates. Unlike the CSSM, TOPS transforms the signal subspace from a reference frequency f_c such that it projects onto the array manifold corresponding to other frequency bins. The orthogonality of this projected signal subspace with the noise subspace of frequency bins under consideration is observed for each direction. Apart from the source directions, this orthogonality is not maintained during DOA estimation. The performance of this technique is found to be superior over CSSM for mid SNR ranges. However, it is mentioned in [12] that this method is highly sensitive to any errors in estimating the number of sources present.

Besides frequency-domain techniques, a wideband technique which estimates source directions by processing data in the time domain has been proposed [13]. This algorithm first reformulates the narrowband-MUSIC algorithm as a beamformer which generates nulls along the source directions. The algorithm subsequently introduces wideband constraints to widen the nulls over a band of frequencies. As will be shown in Section 4, this method is sensitive to the signal subspace dimension chosen.

It is observed that all the above discussed techniques are directly or indirectly dependent on the accuracy in estimating the number of sources. In the literature, several techniques based on information theoretic criteria to estimate the number of sources have been proposed. These algorithms include the Akaike Information Criterion (AIC) and the Minimum Description Length (MDL) [14]. As highlighted in [15], these techniques are suitable for the narrowband case and cease to function in the presence of broadband sources. Performance of broadband DOA estimation deteriorates when operating in conjunction with model order estimation techniques having mediocre performance in low SNR regions (for e.g. [16]). In [17], the source count detection problem is formulated as a multiple hypothesis test. While the performance is superior at low SNR values, the computational complexity involved is immense.

Although model order is one of the outcomes of CSSM technique, the DOA estimation performance is highly sensitive to the initial direction estimates. Using this technique for estimating only the model order is therefore not optimal. In [18], Chung et al., propose a modified maximum likelihood (ML) approach with a maximally hypothesized search followed by a multiple hypothesis testing in order to simultaneously estimate model order and the parameters in wideband source scenario. Although this max-search approach avoids evaluating ML estimates over all possible model orders, the computations involved in obtaining ML estimates is proportional to the number of sensors and maximally hypothesized the number of sources (which is greater than the true model order M).

In wireless communication applications, undesirable phenomena such as multipath and scattering prevail. The signal model defined in (1) does not cater to such situations. While such problems are beyond the scope of this paper interested readers may refer to [19,20] for a different signal model and DOA estimation algorithms developed for such scenarios.

To summarize, the wideband DOA estimation techniques based on spatio-frequency data processing (for e.g. CSSM, TOPS, [18]) require a large number of snapshots. These techniques and that presented in [13] are susceptible to errors in estimating the number of sources. While the solutions for estimating the number of sources are available [16–18], the algorithms are computationally expensive for real-time processing. In a unified system consisting of model order estimator followed by a wideband DOA estimator, the order estimation error can significantly deteriorate the performance of the system in providing DOA estimates. In view of these issues, we propose a new wideband DOA estimation algorithm which provides distinct peaks in the spatial spectrum without knowing a priori the number of sources present. The performance of the proposed estimator is studied with numerical simulations.

The paper is organized as follows. Section 2 provides the required background on the beamformer structure for DOA estimation. Section 3 explains the proposed method for wideband DOA estimation. Section 4 provides the numerical simulations and related discussions. The paper is concluded in Section 5.

2. Beamformer framework for DOA estimation

The power spectrum of the well-known narrowband minimum variance distortionless response (MVDR) beamformer [21] is given by

$$\mathbf{P}_{MVDR}(\theta) = \frac{1}{\mathbf{a}^H(\theta)\mathbf{R}^{-1}\mathbf{a}(\theta)}, \tag{2}$$

where $\mathbf{a}(\theta)$ is the steering vector along the direction θ and $\mathbf{R}$ is the data correlation matrix. This power spectrum $\mathbf{P}_{MVDR}(\theta)$ exhibits peaks corresponding to the source directions. Likewise, the narrowband MUSIC algorithm can also be formulated in the framework of a beamformer as [13]

$$\underset{\mathbf{w}(\theta)}{\text{minimize}} \|\mathbf{w}(\theta) - \mathbf{a}(f_0,\theta)\|_2^2$$
$$\text{subject to } \mathbf{E}_s^H\mathbf{w}(\theta) = 0, \tag{3}$$

where $\mathbf{w}(\theta)$ is the beamformer weight vector corresponding to the look direction θ, $\mathbf{E}_s = [\mathbf{e}_1, \ldots, \mathbf{e}_M]$ is the matrix consisting of M signal subspace eigenvectors of $\mathbf{R}$ and $\mathbf{a}(f_0,\theta)$ is the steering vector defined by

$$\mathbf{a}(f_0,\theta) = [\exp(j\mathbf{k}_\theta^T\mathbf{r}_1), \ldots, \exp(j\mathbf{k}_\theta^T\mathbf{r}_L)]^T, \tag{4}$$

with $\mathbf{r}_i$ and $\mathbf{k}_\theta$ denoting the ith sensor location vector and the wave number vector corresponding to the direction θ at frequency f_0, respectively. While the constraints of (3)

impose the weight vector to reside in the noise subspace, the objective function minimizes the Euclidean distance between the weight vector $\mathbf{w}(\theta)$ and the steering vector $\mathbf{a}(f_0,\theta)$. The solution to the optimization problem in (3) is shown in [13] to be $\mathbf{w}(\theta)=\mathbf{E}_n\mathbf{E}_n^H\mathbf{a}(f_0,\theta)$, with $\mathbf{E}_n$ denoting the noise subspace of $\mathbf{R}$. As a result, (3) produces nulls in the MUSIC null-spectrum function $|\mathbf{w}^H(\theta)\mathbf{a}(f_0,\theta)|$ along source directions. Source directions can therefore be estimated from the peaks of the direction finding function

$$DF(\theta)=\frac{1}{|\mathbf{w}^H(\theta)\mathbf{a}(f_0,\theta)|}=\frac{1}{\|\mathbf{E}_n^H\mathbf{a}(f_0,\theta)\|_2^2}. \tag{5}$$

We note that the steering vector for a given direction is a continuous function of frequency. The method in [13] imposes additional linear constraints

$$\begin{aligned}&\mathbf{w}^H(\theta)\frac{\partial\mathbf{a}(f,\theta)}{\partial f}\bigg|_{f=f_0}=0,\\ &\mathbf{w}^H(\theta)\frac{\partial^2\mathbf{a}(f,\theta)}{\partial f^2}\bigg|_{f=f_0}=0,\\ &\quad\vdots\end{aligned} \tag{6}$$

in order to make the weight vector insensitive to the frequency variations along the direction θ. By imposing these derivative constraints, the weight vector $\mathbf{w}(\theta)$ regulates the null width of the array response along the frequency axis. We refer to this technique as Beamformer Framework Wideband MUSIC (BFW-MUSIC) algorithm in this paper.

Some of the interesting features of this technique are:

- Reduced number of time-domain snapshots required for DOA estimation in comparison with the frequency-domain techniques such as CSSM [5] and TOPS [12].
- Robustness to the deviation of source center frequency achieved by widening the null width.
- Capability to estimate directions of varying bandwidth sources.

It is important to note that this MUSIC formulation requires the signal subspace of the time-domain auto-correlation matrix. While the presence of wideband sources disposes the notion of signal subspace and noise subspace in time domain, experiments reveal that a subspace with eigenvectors corresponding to dominant eigenvalues yield acceptable DOA estimates. However, the choice of this subspace dimension $\dim\{\mathbf{E}_s\}$ is not discussed in [13].

To illustrate the effect of the choice of $\dim\{\mathbf{E}_s\}$ on the spatial spectrum of BFW-MUSIC algorithm, we consider a 10-element double-ring array receiving data from three wideband sources located at 30°, 45° and 70°. With the sampling frequency normalized to $f_s=1$, the sources have a center frequency equal to $f_c=0.3$ and have a normalized bandwidth of 0.15, respectively. The number of snapshots used to form the correlation matrix is 500. The spatial spectrum in Fig. 1 shows that the source directions are accurately estimated for only limited cases. While the resolution degrades with smaller choice of $\dim\{\mathbf{E}_s\}$, overestimation results in additional false peaks along other directions, as seen for the case of $\dim\{\mathbf{E}_s\}=7$. The strong

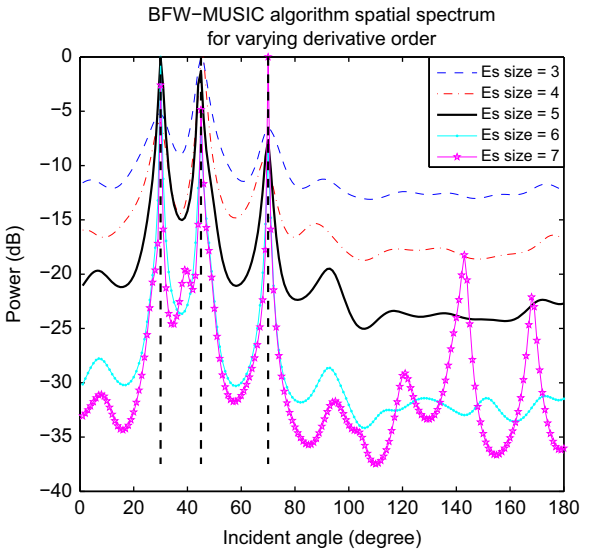

Fig. 1. Spatial spectrum of Wideband MUSIC algorithm for varying signal subspace size.

dependence on signal subspace dimension therefore limits the performance of the algorithm under practical conditions. The use of MDL and AIC was verified to yield inconsistent signal subspace dimensionality. Therefore, it is of interest to consider an alternative formulation which does not rely on the model order.

3. Proposed method

The formulation of narrowband MUSIC algorithm in (3) has first order equality constraints. While these constraints ensure weight vector to be orthogonal to the signal subspace, the objective function minimizes the Euclidean distance between $\mathbf{w}(\theta)$ and $\mathbf{a}(\theta)$ in the L-dimensional vector space along each direction θ. In [22], a MUSIC-like algorithm is developed based on beamforming framework for narrowband DOA estimation. The performance of this algorithm approaches that of narrowband MUSIC even without knowing the number of sources a priori. The constrained optimization problem solved in this algorithm is given by

$$\begin{aligned}&\underset{\mathbf{w}}{\text{minimize}}\ \mathbf{w}^H\mathbf{R}\mathbf{w}\\ &\text{subject to}\ \mathbf{w}^H\{\mathbf{a}(f_0,\theta)\mathbf{a}^H(f_0,\theta)+\beta\mathbf{I}\}\mathbf{w}=c,\end{aligned} \tag{7}$$

where $\beta,c>0$ are constants while $\mathbf{I}$ is the identity matrix. For notational convenience, the argument of the weight vector $\mathbf{w}$ has been dropped although it is direction dependent. The solution to this problem is given by the eigenvector corresponding to the minimum eigenvalue $\lambda_{\min}$ of the generalized eigenvalue (GEV) problem

$$\mathbf{R}\mathbf{w}=\lambda_{\min}\{\mathbf{a}(f_0,\theta)\mathbf{a}^H(f_0,\theta)+\beta\mathbf{I}\}\mathbf{w}.$$

In order to provide an insight to the optimization problem in (7), we decompose the objective function as

$$\mathbf{w}^H\mathbf{R}\mathbf{w}=\mathbf{w}^H\mathbf{R}_s\mathbf{w}+\mathbf{w}^H\mathbf{R}_n\mathbf{w}, \tag{8}$$

where $\mathbf{R}_s = \mathbf{A}(f_0,\Theta)\mathbf{R}_{ss}\mathbf{A}^H(f_0,\Theta)$ denotes the source contribution to $\mathbf{R}$, while $\mathbf{R}_{ss} = \mathrm{E}\{\mathbf{s}(n)\mathbf{s}^H(n)\}$ and $\mathbf{R}_n = \mathrm{E}\{\mathbf{v}(n)\mathbf{v}^H(n)\}$ denote the source and noise covariance matrices, respectively. With constant noise power across all sensors, it is interesting to note that the second term remains a constant. Therefore, the minimization of objective function minimizes only the projection of the weight vector onto the signal subspace. As a consequence, the weight vector resides in the noise subspace. Along the non-source directions, due to the imposed constraint, the solution weight vector $\mathbf{w}$ spans $\mathrm{sp}\{\mathbf{E}_n\} \cap \mathrm{sp}\{\mathbf{a}(f_0,\theta),\ \forall\theta \notin \Theta\}$, where sp $\{\cdot\}$ denotes the subspace spanned, resulting in $|\mathbf{w}^H\mathbf{a}(f_0,\theta)| \neq 0$. However, along the source directions, it is known that the steering vectors $\mathbf{a}(f_0,\Theta)$ span only the signal subspace $\mathbf{E}_s$. With weight vector spanning only the noise subspace, we have $\mathrm{sp}\{\mathbf{E}_n\} \cap \mathrm{sp}\{\mathbf{a}(f_0,\theta),\ \forall\theta \in \Theta\} = \emptyset$, which produces peaks in $DF(\theta)$ along the source directions.

In the wideband signal model described by (1), the array manifold matrix $\mathbf{A}(f,\Theta)$ varies with frequency. The steering vector corresponding to the source direction θ_0 at frequency f is given by

$$\mathbf{a}(f,\theta_0) = \left[\exp\left(j\frac{2\pi f}{v}\mathbf{v}_{\theta_0}^T\mathbf{r}_1\right),\ldots,\exp\left(j\frac{2\pi f}{v}\mathbf{v}_{\theta_0}^T\mathbf{r}_L\right)\right]^T, \tag{9}$$

where $\mathbf{k}_{\theta_0} = (2\pi f/v)\mathbf{v}_{\theta_0}$ is the wave number vector with v denoting the propagation speed and $\mathbf{v}_{\theta_0}$ the source direction vector. Although the steering vector changes with frequency for wideband sources, we obtain a relation for data snapshots in time domain. Over the time frame indexed l, the signal model defined in (1) can be introduced into the inverse discrete Fourier transform (DFT) relation to obtain

$$\mathbf{x}(n) = \frac{1}{K}\sum_{k=0}^{K-1}\mathbf{x}(f_k,l)e^{j2\pi kn/K} = \frac{1}{K}\sum_{k=0}^{K-1}\mathbf{A}(f_k,\Theta)\mathbf{s}(f_k,l)e^{j2\pi kn/K} + \mathbf{v}(n), \tag{10}$$

where $\mathbf{v}(n)$ is the additive noise vector uncorrelated with the sources, f_k is the frequency in the kth bin and K is the order of DFT. Following the derivation provided in Appendix A, the time-domain data covariance matrix is given by

$$\begin{aligned}\mathbf{R} &= \mathrm{E}\{\mathbf{x}(n)\mathbf{x}^H(n)\}\\ &= \frac{1}{K^2}\mathbf{A}(f_0,\Theta)\left\{\sum_{k=0}^{K-1}\mathbf{R}_{ss}(f_k)\right\}\mathbf{A}^H(f_0,\Theta)\\ &\quad + \frac{1}{K^2}\sum_{k=0}^{K-1}\sum_{p=1}^{P}\frac{(\Delta f_k)^{2p}}{p!^2}\frac{\partial^p}{\partial f^p}\mathbf{A}(f,\Theta)\Big|_{f=f_0}\\ &\quad \mathbf{R}_{ss}(f_k)\frac{\partial^p}{\partial f^p}\mathbf{A}^H(f,\Theta)\Big|_{f=f_0} + \sigma_v^2\mathbf{I},\end{aligned} \tag{11}$$

where $\mathbf{R}_{ss}(f)$ is the source covariance matrix at frequency f, P is the order of Taylor series expansion and σ_v^2 is the noise variance. It is interesting to observe that the derivative constraints in (6) suppress the additional derivative terms in $\mathbf{R}$ except for the narrowband component at f_0.

3.1. Formulation

For narrowband sources, the objective function of (7) minimizes the beamformer output power. In what follows, we introduce another quadratic term into the objective function which minimizes the projection of $\mathbf{w}$ onto the space spanned by the steering vector derivatives w.r.t. frequency. The idea here is to suppress the derivative components in (11), thus reducing it to a narrowband autocorrelation matrix obtained for sources at frequency f_0.

To achieve the above, we first define a matrix $\mathbf{D}_{f_0,\theta}$ consisting of unit norm derivatives of the steering vector w.r.t. frequency up to the order of P as its columns,

$$\mathbf{D}_{f_0,\theta} = [\tilde{\mathbf{d}}_1(f_0,\theta)\ \tilde{\mathbf{d}}_2(f_0,\theta)\ \ldots\ \tilde{\mathbf{d}}_P(f_0,\theta)], \tag{12}$$

where $\tilde{\mathbf{d}}_l(f_0,\theta) = \mathbf{d}_l(f_0,\theta)/\|\mathbf{d}_l(f_0,\theta)\|_2$ and $\mathbf{d}_l(f_0,\theta) = \partial^l\mathbf{a}(f,\theta)/\partial f^l|_{f=f_0}$. For consistency, we also maintain $\|\mathbf{a}(\theta)\|_2^2 = 1$ henceforth. The projection matrix of $\mathbf{D}_{f_0,\theta}$ is given by

$$\mathbf{P}_{\mathbf{D}_\theta} = \mathbf{D}_{f_0,\theta}(\mathbf{D}_{f_0,\theta}^H\mathbf{D}_{f_0,\theta})^{-1}\mathbf{D}_{f_0,\theta}^H,$$

which spans the same subspace as that of $\mathbf{D}_{f_0,\theta}$. Premultiplication of sensor snapshots $\mathbf{x}(n)$ with $\mathbf{P}_{\mathbf{D}_\theta}$ projects the data onto the derivative vector space, $\mathbf{y}_\theta(n) = \mathbf{P}_{\mathbf{D}_\theta}\mathbf{x}(n)$, which can be loosely termed as derivative transformed data snapshots. The autocorrelation matrix of $\mathbf{y}_\theta(n)$ is then given by

$$\mathbf{R}_y(\theta) = \mathrm{E}\{\mathbf{y}_\theta(n)\mathbf{y}_\theta^H(n)\} = \mathbf{P}_{\mathbf{D}_\theta}\mathbf{R}\mathbf{P}_{\mathbf{D}_\theta}^H. \tag{13}$$

It is important to note that the eigenvectors of $\mathbf{R}_y(\theta)$ spans only the derivative vector space. This implies that the minimization of the term $\mathbf{w}^H\mathbf{R}_y(\theta)\mathbf{w}$ is an alternative approach to achieve the functionality of the constraints in (6). Furthermore, the eigenvalues of $\mathbf{R}_y(\theta)$ are data-dependent and provides appropriate weighting for the derivative constraints. Therefore, we introduce this term into the objective function resulting in a new optimization problem

$$\begin{aligned}&\underset{\mathbf{w}}{\text{minimize}} \quad \mathbf{w}^H\mathbf{R}\mathbf{w} + \zeta\mathbf{w}^H\mathbf{R}_y(\theta)\mathbf{w}\\ &\text{subject to} \quad \mathbf{w}^H\{\mathbf{a}(f_0,\theta)\mathbf{a}^H(f_0,\theta) + \beta\mathbf{I}\}\mathbf{w} = c,\end{aligned} \tag{14}$$

where $\zeta,\beta,c > 0$ are constants discussed subsequently. The solution to this problem can be obtained by setting the gradient of the Lagrangian function

$$\begin{aligned}L(\mathbf{w},\lambda) &= \mathbf{w}^H(\mathbf{R} + \zeta\mathbf{R}_y(\theta))\mathbf{w}\\ &\quad -\lambda(\mathbf{w}^H\mathbf{a}(f_0,\theta)\mathbf{a}^H(f_0,\theta)\mathbf{w} + \beta\|\mathbf{w}\|_2^2 - c)\end{aligned} \tag{15}$$

with respect to the conjugate of $\mathbf{w}$ equal to zero. Here λ is the Lagrangian multiplier. The optimal weight vector for a given direction is obtained as the eigenvector corresponding to the minimum eigenvalue ($\lambda_{\min}$) of the generalized eigenvalue (GEV) problem,

$$(\mathbf{R} + \zeta\mathbf{R}_y(\theta))\mathbf{w} = \lambda_{\min}(\mathbf{a}(f_0,\theta)\mathbf{a}^H(f_0,\theta) + \beta\mathbf{I})\mathbf{w}. \tag{16}$$

Since the solution weight vector is independent of c, its value need not be determined. However, for any $\beta > 0$, the matrix $\mathbf{a}(f_0,\theta)\mathbf{a}^H(f_0,\theta) + \beta\mathbf{I}$ is positive definite enforcing $c > 0$ from the constraint.

The bounds derived for β in the narrowband case [22] cannot be extended to this formulation since the correlation matrix in the objective function changes for each direction.

We therefore discuss on the choice of β and ζ in the next subsection.

3.2. Choice of parameters

We start with the discussion on the choice of β by setting $\zeta=1$. The solution for (14) can alternatively be written as

$$(\mathbf{a}(f_0,\theta)\mathbf{a}^H(f_0,\theta)+\beta\mathbf{I})\mathbf{w}=\hat{\lambda}_{\max}(\mathbf{R}+\mathbf{R}_y(\theta))\mathbf{w}, \tag{17}$$

where $\hat{\lambda}_{\max}=1/\lambda_{\min}$ is the maximum eigenvalue of the matrix pencil $\{\mathbf{a}(f_0,\theta)\mathbf{a}^H(f_0,\theta)+\beta\mathbf{I},\mathbf{R}+\mathbf{R}_y(\theta)\}$ and the solution $\mathbf{w}$ is the corresponding generalized eigenvector. With $\mathbf{R}+\mathbf{R}_y(\theta)$ being positive definite, (17) takes the form

$$(\mathbf{R}+\mathbf{R}_y(\theta))^{-1}(\mathbf{a}(f_0,\theta)\mathbf{a}^H(f_0,\theta)+\beta\mathbf{I})\mathbf{w}=\hat{\lambda}_{\max}\mathbf{w},$$

$$\{\mathbf{A}+\beta\mathbf{B}\}\mathbf{w}=\hat{\lambda}_{\max}\mathbf{w}, \tag{18}$$

where $\mathbf{B}=(\mathbf{R}+\mathbf{R}_y(\theta))^{-1}$ and $\mathbf{A}=\mathbf{B}\mathbf{a}(f_0,\theta)\mathbf{a}^H(f_0,\theta)$. We hence have

$$\mathbf{w}^H\{\mathbf{A}+\beta\mathbf{B}\}\mathbf{w}=\hat{\lambda}_{\max}\|\mathbf{w}\|_2^2, \tag{19}$$

$$\frac{\mathbf{w}^H\{\mathbf{A}+\beta\mathbf{B}\}\mathbf{w}}{\|\mathbf{w}\|_2^2}=\hat{\lambda}_{\max}. \tag{20}$$

For DF(θ) to provide peaks along source directions, $\mathbf{w}$ has to satisfy $|\mathbf{w}^H\mathbf{a}(f_0,\theta)|=0$. This requires asymptotically $\mathbf{A}\mathbf{w}=\mathbf{B}\mathbf{a}(f_0,\theta)\mathbf{a}^H(f_0,\theta)\mathbf{w}=0$, and therefore β has to be chosen such that

$$\frac{\mathbf{w}^H\mathbf{A}\mathbf{w}}{\|\mathbf{w}\|_2^2}\ll\beta\frac{\mathbf{w}^H\mathbf{B}\mathbf{w}}{\|\mathbf{w}\|_2^2}. \tag{21}$$

The expressions on either sides of (21) are the eigenvalues of $\mathbf{A}$ and $\mathbf{B}$. Since $\hat{\lambda}_{\max}$ corresponds to the maximum eigenvalue of $\{\mathbf{A}+\beta\mathbf{B}\}$, the choice of $\mathbf{w}$ which maximizes either sides of (21) correspond to the maximum eigenvalue

$$\beta\gamma_{\max}(\mathbf{B})\gg\gamma_{\max}(\mathbf{A}),\quad\forall\theta\in\Theta, \tag{22}$$

where $\gamma_{\max}(\mathbf{A})$ and $\gamma_{\max}(\mathbf{B})$ are the maximum eigenvalues of $\mathbf{A}$ and $\mathbf{B}$. Since tr $\{\mathbf{A}\}>\gamma_{\max}(\mathbf{A})$, we rewrite the above relation w.r.t. the trace of $\mathbf{A}$ as

$$\beta>\frac{\mathrm{tr}\{\mathbf{A}\}}{\gamma_{\max}(\mathbf{B})}>\frac{\gamma_{\max}(\mathbf{A})}{\gamma_{\max}(\mathbf{B})},\quad\forall\theta\in\Theta. \tag{23}$$

Exploiting the identity, $\mathrm{tr}\{\mathbf{EFG}\}=\mathrm{tr}\{\mathbf{GEF}\}$, for any three matrices $\mathbf{E}$,$\mathbf{F}$ and $\mathbf{G}$ [23], (23) can be rewritten as

$$\beta>\frac{\mathrm{tr}\{\mathbf{B}\mathbf{a}(f_0,\theta)\mathbf{a}^H(f_0,\theta)\}}{\gamma_{\max}(\mathbf{B})}=\frac{\mathbf{a}^H(f_0,\theta)\mathbf{B}\mathbf{a}(f_0,\theta)}{\gamma_{\max}(\mathbf{B})},\quad\forall\theta\in\Theta. \tag{24}$$

In order to provide a better insight to this lower bound, we plot the numerator of (24) as a function of θ in Fig. 2 for an example with three sources along 30°,40° and 60°. It is interesting to note that this function is the reciprocal of the MVDR power spectrum with $\mathbf{R}+\mathbf{R}_y(\theta)$ used as the correlation matrix and has minima along the source directions while in all other directions the amplitude is relatively large. For the proposed technique, peaks along source directions are assured for all β greater than the minima of $\mathbf{a}^H(f_0,\theta)\mathbf{B}\mathbf{a}(f_0,\theta)/\gamma_{\max}(\mathbf{B})$.

For directions $\theta\notin\Theta$, we require $\mathbf{A}\mathbf{w}\neq0$ to avoid any possible false peaks in the spatial spectrum. In view of this, β cannot be arbitrarily high and has to be constrained such that the solution $\mathbf{w}$ is obtained with comparable contributions from $\mathbf{A}$ and $\mathbf{B}$ in (18). From Fig. 2, we note that $\gamma_{\max}(\mathbf{B})>\gamma_{\max}(\mathbf{A}),\forall\theta$. In order to reduce the influence of $\mathbf{B}$ in (18), β can be constrained such that

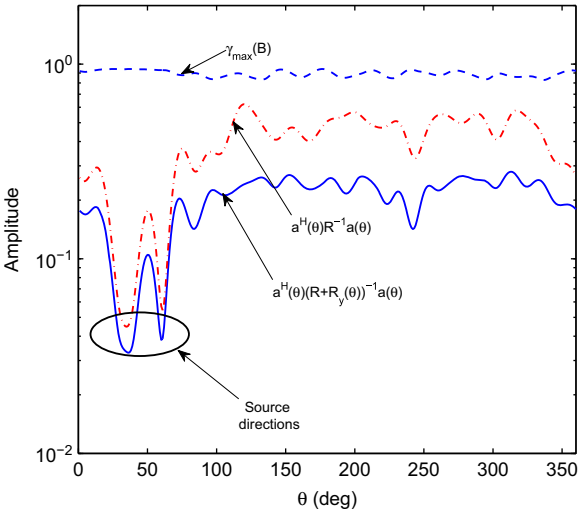

Fig. 2. Plot of $\mathbf{a}^H(f_0,\theta)(\mathbf{R}+\mathbf{R}_y(\theta))^{-1}\mathbf{a}(f_0,\theta)$ and $\mathbf{a}^H(f_0,\theta)\mathbf{R}^{-1}\mathbf{a}(f_0,\theta)$ when three sources are present.

$$\beta<\max_\theta\frac{\mathbf{a}^H(f_0,\theta)\mathbf{B}\mathbf{a}(f_0,\theta)}{\gamma_{\max}(\mathbf{B})}. \tag{25}$$

Therefore, β is bound by

$$\min_\theta\frac{\mathbf{a}^H(f_0,\theta)\mathbf{B}\mathbf{a}(f_0,\theta)}{\gamma_{\max}(\mathbf{B})}<\beta<\max_\theta\frac{\mathbf{a}^H(f_0,\theta)\mathbf{B}\mathbf{a}(f_0,\theta)}{\gamma_{\max}(\mathbf{B})}. \tag{26}$$

A good choice for β can hence be obtained from the mean of the function $\mathbf{a}^H(f_0,\theta)\mathbf{B}\mathbf{a}(f_0,\theta)$. However, with $\mathbf{B}$ being direction dependent, matrix inversion in each direction is computationally expensive. In order to reduce the complexity required to estimate β, we study the function $\mathbf{a}^H(f_0,\theta)\mathbf{R}^{-1}\mathbf{a}(f_0,\theta)$ plotted in Fig. 2. This function corresponds to the case when $\zeta=0$. We note that the minima of this function coincides approximately with that of $\mathbf{a}^H(f_0,\theta)\mathbf{B}\mathbf{a}(f_0,\theta)$ along the source directions, while in all other directions, it has a higher value than $\mathbf{a}^H(f_0,\theta)\mathbf{B}\mathbf{a}(f_0,\theta)$. Therefore, β can be chosen as

$$\beta=\eta\frac{\mathrm{mean}\{\mathbf{a}^H(f_0,\theta)\mathbf{R}^{-1}\mathbf{a}(f_0,\theta)\}}{\gamma_{\max}(\mathbf{R}^{-1})}, \tag{27}$$

where $0<\eta<1$ assures reliable DOA estimates and mean$\{\cdot\}$ denotes the mean of the function over θ.

It is important to note that the function in the numerator (27) is the reciprocal of the MVDR beamformer power response which is being used to determine the value of β. Fig. 3 shows the plot of the function $g(\theta)=\mathbf{a}^H(f_0,\theta)\mathbf{R}^{-1}\mathbf{a}(f_0,\theta)/\gamma_{\max}(\mathbf{R}^{-1})$. The figure also illustrates the values of β for various η. We note that the value of β for $\eta\leq0.5$ can segregate the angular sections consisting of source directions from other directions. Therefore, this provides good diagonal loading value in the constraint of (14). The sensitivity of this parameter over the DOA estimates is studied in the next section.

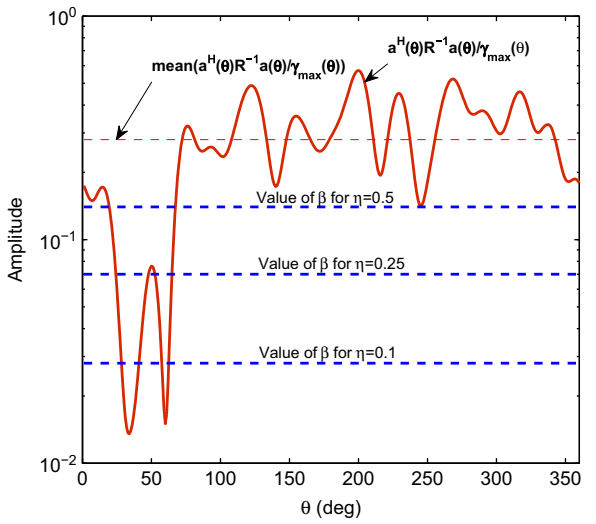

Fig. 3. Plot of $g(\theta)$ and the value of β for various values of η.

The parameter ζ regulates the contribution of the derivative data snapshots in the objective function of (14). The term $\mathbf{w}^H\mathbf{R}_y(\theta)\mathbf{w}$ provides additional weight along source directions to suppress the derivative components than in other directions. The autocorrelation matrix $\mathbf{R}_y(\theta)$ is obtained from the data snapshots projected onto the derivative vector space of $\mathbf{a}(f_0,\theta)$. However, the P derivative vectors used to construct the projection matrix $\mathbf{P}_{\mathbf{D}_\theta}$ spans a subspace of the L-dimensional data space. Therefore, the matrix $\mathbf{R}_y(\theta)$ does not vanish in the presence of only narrowband sources. In order to regulate the contribution of $\mathbf{R}_y(\theta)$ with the signal bandwidth, the parameter ζ has to be chosen based on the signal bandwidth. While a low value of ζ subside the effectiveness of the constraint, a very high value will outweigh $\mathbf{R}_y(\theta)$ over $\mathbf{R}$. Therefore, we provide the following range for ζ:

$$\frac{BW}{f_c} \le \zeta < 1, \tag{28}$$

where BW and f_c are the bandwidth and center frequency of the sources present in the scenario, respectively. This bound is obtained with an intuitive understanding that, the lower limit reduces to $\zeta = 0$ in the presence of only the narrowband sources, in which case the formulation resembles the narrowband MUSIC-like algorithm in (7). On the contrary, the upper limit of $\zeta = 1$ assigns equal weights to both $\mathbf{R}$ and $\mathbf{R}_y(\theta)$ when the fractional bandwidth $BW/f_c \ge 1$. In Section 4, we study the sensitivity of DOA estimation performance with the choice of ζ for various SNR values.

Note that the formulation of (14) is similar to the optimization problem in [24] proposed for adaptive beamforming with robustness against jammer motion. While the technique in [24] imposes derivative constraints w.r.t. the wavenumber to achieve invariance in the spatial spectrum around a given source direction θ, the proposed technique imposes derivative constraints w.r.t. frequency so that $\mathbf{w}$ is invariant to the steering vector variations around the center frequency f_0.

3.3. Computational complexity

Evaluating the precise computational complexity for the proposed technique involves computation of the steering vector derivatives, matrix multiplication and solving a GEV problem for each direction. With steering vector derivatives independent of data, run-time computational load can be reduced significantly with a look-up to values evaluated a priori. Therefore, solving GEV in each direction is the run-time computationally intensive task. Rao et. al. [25] proposed an iterative algorithm to realize generalized eigendecomposition with a computational complexity of $O(L^2)$. Including the computation of matrix inversion and maximum eigenvalue of $\mathbf{R}^{-1}$ required for setting β (which together consumes $O(L^3)+O(L^2)$), the total computational load of the proposed technique is $O(L^3)+(N_{\text{tot}}+1)O(L^2)$, where N_{tot} is the number of search directions.

The BFW-MUSIC algorithm requires the inversion of a $D\times D$ matrix ($D=\dim(\mathbf{E}_s)+P$) in each direction. Besides ignoring the computational cost involved in the estimation of the signal subspace dimension, the $O(D^3)$ matrix inversion operation results in a total complexity of $N_{\text{tot}}O(D^3)$. Although $D<L$, the third degree complexity indicates an increase in complexity with increasing signal subspace dimension. The TOPS algorithm requires an eigendecomposition of the $L\times L$ autocorrelation matrix in each frequency bin, followed by an eigendecomposition of a smaller $P\times P$ matrix in each direction. This results in a total computational complexity of $N_{\text{bins}}O(L^2)+N_{\text{tot}}O(P^2)$, where N_{bins} is the number of frequency bins used. This is again a conservative measure without considering the computations required for estimating the model order. While the CSSM technique requires to solve a single SVD for DOA estimation, the process of finding the focussing matrices requires an $L\times L$ matrix SVD in each frequency bin of consideration. Although this technique is computationally less intensive, it additionally requires an initial estimate of the source directions obtained from another technique. Comparing the complexity of the model order estimation techniques and the prerequisites required for the CSSM algorithm, the proposed technique has marginal advantage in terms of computation.

4. Numerical results and discussions

All the numerical experiments are performed for a double-ring array of 10 elements ($L=10$) shown in Fig. 4 with the array phase center coinciding with the origin of the coordinate system. The source azimuths are measured from the horizontal x-axis. Despite the radius of the two rings being greater than $\lambda/2$, the farfield planar wavefront from any source direction is sampled by a set of sensors complying with the $\lambda/2$ phase delay, thus avoiding any source direction ambiguity due to spatial aliasing. The wideband sources are generated as a sum of sinusoids with random phase and magnitude within the bandwidth,

$$s(t) = \sum_{i=1}^{D} a_i \exp\{\jmath(2\pi f_i t + c_i(t))\}, \tag{29}$$

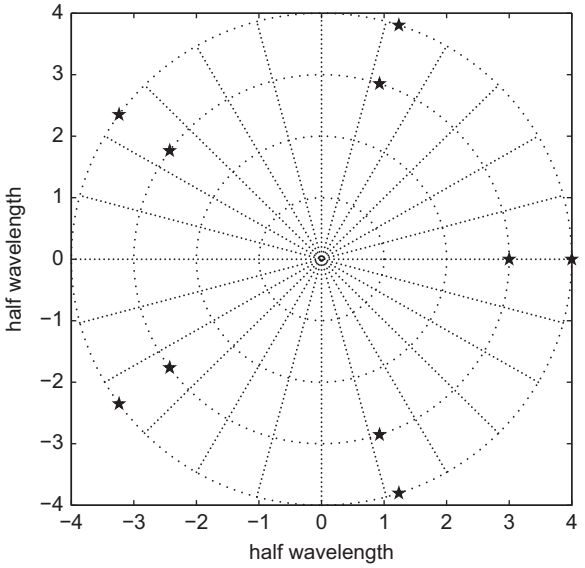

Fig. 4. Ten-element double ring circular array.

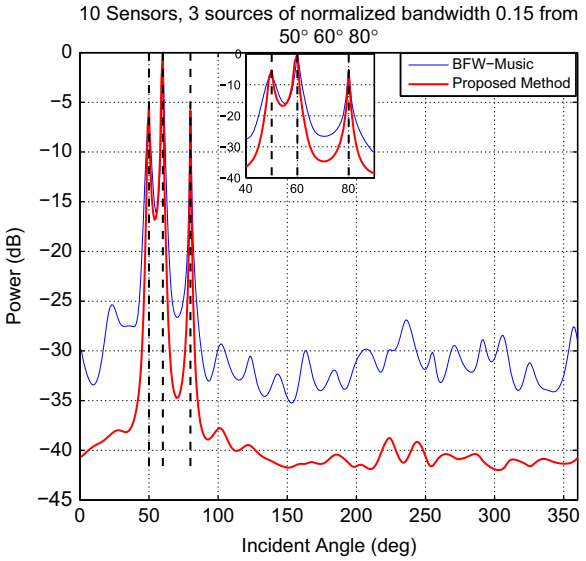

Fig. 5. Spatial spectrum of BFW-MUSIC algorithm and the proposed technique.

where the amplitude a_i is an instance of Rayleigh distribution, $c_i(t)$ is uniformly distributed in $[-\pi,\pi]$ and D is the number of sinusoids that constitute the wideband source, or effectively, the bandwidth of the sources. For all the experiments in this section, the bandwidth of wideband sources is specified with their normalized bandwidths given by BW/f_s, where f_s is the sampling frequency. Additive complex Gaussian noise is used to generate sensor data snapshots at required SNR in accordance with the signal model defined in (1).

For illustration purposes, we choose $\zeta = 0.75 < 1$ and $\eta = 0.5$ to satisfy the condition given in (28). A discussion on the choice of these parameters will be presented in the sequel. For BFW-MUSIC algorithm, the signal subspace dimension $\dim\{\mathbf{E}_s\}$ has to be chosen as the number of significant eigenvalues in the autocorrelation matrix. However, based on a Monte Carlo study of the spatial spectrum for various scenarios, $\dim\{\mathbf{E}_s\} = M+2$, where M is the number of sources, has been chosen to obtain a good spatial spectrum without false peaks.

In the first experiment, three wideband sources are positioned at 50°, 60° and 80° in the far-field. The spatial spectrum for the proposed method and the BFW-MUSIC algorithm is shown in Fig. 5. For BFW-MUSIC algorithm, $\dim\{\mathbf{E}_s\} = M+2 = 5$ was chosen. With sampling frequency normalized to unity, the sources are centered at $f_c = 0.3$ and have equal normalized bandwidths of 0.15. The SNR and the number of data snapshots used are 10 dB and 500, respectively. Fig. 5 demonstrates that the proposed technique can provide peaks along the source directions without knowing the number of sources. We notice that the spatial spectrum does not exhibit any false peaks along non-source directions.

It is essential to study the effect of derivative order P used in estimating $\mathbf{R}_y(\theta)$ for the proposed technique. For BFW-MUSIC, an increase in the number of derivative constraints adversely affects the degrees of freedom available for the weight vector solution. Whereas for the proposed technique, the derivative conditions are imposed in the form of $\mathbf{R}_y(\theta)$. This results in a data dependent weighting for the derivative constraints and hence the choice of derivative order should not significantly affect the performance. To validate this understanding, we performed an experiment with three equal bandwidth sources (normalized bandwidth = 0.15) from 50°, 70° and 80° with the same SNR and number of snapshots as the previous experiment. The order of derivative vectors is increased from 1 to 4. Fig. 6(a) shows the variation of spatial spectrum for varying derivative orders. We observe that the spatial spectrum of BFW-MUSIC algorithm yields good source direction estimates till the derivative order is increased to 3. When the order is 4, we observe false peaks in the spectrum which in this case, the weight vector has only one degree of freedom (with $P = 4$ and $\dim\{\mathbf{E}_s\} = 5$). On the contrary, we observe from Fig. 6(b) that the proposed technique is not significantly affected by the derivative vector order. This experiment highlights the robustness of the proposed technique for the choice of P.

The formulation of proposed technique incorporates parameters such as β and ζ. The study of the DOA estimation performance over these parameters is conducted with the root mean squared error (RMSE) of the source direction estimate plotted against these parameters for various SNR values. In the first experiment, we fixed $\zeta = 0.75$ and varied the value of η which in turn regulates the diagonal loading value β. Fig. 7(a) shows the RMSE of the DOA estimates for the same setup as in the previous experiment. For moderate and high SNR conditions, we observe that the proposed technique is not significantly affected by the choice of η within the range of [0.3,1.3]. However, at 0 dB SNR, the RMSE decreases

with increasing η until $\eta = 0.3$, beyond which RMSE gradually increases. From this study, we identify $\eta = 0.5$ from the plot for SNR $= 0$ dB to suffice for all other conditions.

With this choice for η, we observe the effect of ζ on the DOA estimates for the same experimental setup. Fig. 7(b) shows the RMSE of DOA estimates plotted against ζ for various SNRs. We note that for $\zeta < 0.3$, it is observed that RMSE for DOA estimates is large. This can be accounted to the fact that the derivative constraints are not completely imposed. When ζ is increased within the bounds provided in (28), the RMSE increases modestly. Although not optimal, we use $\zeta = 0.75$ for the rest of our studies, while choosing a different value provides marginal improvement in performance.

We proceed to evaluate the estimation performance of the proposed technique. We first compare the proposed technique with BFW-MUSIC algorithm as a function of SNR and the number of snapshots. With time-domain snapshots as less as 500–1000, existing frequency domain techniques such as CSSM and TOPS cease to provide DOA estimates and hence cannot be compared. We then compare the performance of the proposed technique with TOPS algorithm [12] which processes data in the frequency domain. Since the performance of CSSM is sensitive to the initial source estimates provided, we limit our comparison to TOPS algorithm alone. Following this, we study the resolution capability of the proposed technique for two closely spaced sources.

Three wideband sources with fractional bandwidth of 0.5 emit signals from 50°, 60° and 80°. Five hundred snapshots are used in each trial for studying the bias, standard deviation and RMSE of the estimate. The performance of the technique in comparison with BFW-MUSIC for all the three sources averaged over 200 trials is detailed in Tables 1 and 2. The BFW-MUSIC algorithm is evaluated for the signal subspace dimensions of 5, 6 and 7. When $\dim\{\mathbf{E}_s\} = 7$ and $P=2$, the solution to the weight vector has only one degree of freedom for the 10 sensor array. Therefore, with $\dim\{\mathbf{E}_s\} = 7$, we also study the case with $P=1$ in order to provide two degrees of freedom for the solution. From Tables 1 and 2, we derive the following conclusions:

- The bias of BFW-MUSIC estimates with $\dim\{\mathbf{E}_s\} = 7$ and $P=2$ is very low compared to other configurations of BFW-MUSIC as well as the proposed technique at lower SNR values. Nevertheless, from Fig. 1, we observe that the spatial spectrum in this case has false peaks which is a direct consequence of the reduced degrees of freedom for the weight vector solution. The DOA estimates obtained from the proposed technique has the next best performance with bias approaching zero at increasing SNR values.

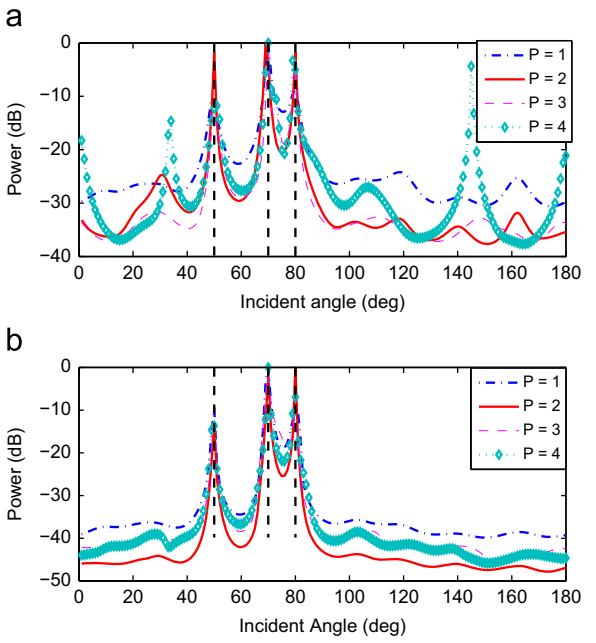

Fig. 6. Spatial spectrum of BFW-MUSIC algorithm and the proposed technique for varying order of derivative constraints. (a) Spatial spectrum of BFW-MUSIC algorithm and (b) Spatial spectrum of Proposed Technique.

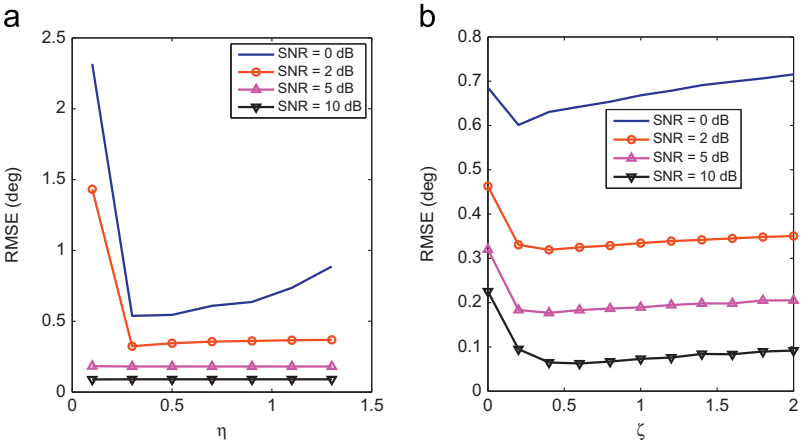

Fig. 7. RMSE of DOA estimates averaged over 50 trials against (a) η, (b) ζ.

Table 1
Bias (deg) of the estimates for DOA=50°,60° and 80°.

SNR (dB)	DOA (deg)	BFW MUSIC (deg)				Proposed method (deg)
		$\mathbf{E}_s=5, P=2$	$\mathbf{E}_s=6, P=2$	$\mathbf{E}_s=7, P=2$	$\mathbf{E}_s=7, P=1$	
0	50	0	0.3646	0.0294	−0.6528	0.2411
	60	−0.129	−0.1215	−0.0441	−0.0139	−0.2482
	80	0.1613	−0.0552	−0.0588	0.4722	−0.0284
10	50	0.0051	0.2412	−0.0213	−1.105	0.075
	60	−0.1624	0.0704	−0.1277	−0.05	−0.1
	80	0.0964	−0.0352	0	0.335	0.005
20	50	−0.0505	0.23	0	−1.085	0
	60	−0.0859	0.13	0.1263	−0.075	−0.025
	80	0.0354	−0.005	−0.0051	0.165	0

Table 2
RMSE (deg) of the estimates for DOA=50°,60° and 80°.

SNR (dB)	DOA (deg)	BFW MUSIC (deg)				Proposed method (deg)
		$\mathbf{E}_s=5, P=2$	$\mathbf{E}_s=6, P=2$	$\mathbf{E}_s=7, P=2$	$\mathbf{E}_s=7, P=1$	
0	50	0.8065	1.0055	1.0441	1.4167	1.0922
	60	0.5484	0.9613	1.4853	1.0833	1.2837
	80	0.4516	0.3978	0.75	0.8472	0.4823
10	50	0.4112	0.2915	0.0745	1.395	0.175
	60	0.203	0.3015	0.8191	0.28	0.46
	80	0.1675	0.0452	0.0106	0.345	0.045
20	50	0.303	0.25	0	1.275	0
	60	0.1162	0.25	0.5808	0.185	0.045
	80	0.1566	0.005	0.0051	0.165	0

- For the case of $\dim\{\mathbf{E}_s\}=7$ and $P=1$, we note that BFW-MUSIC algorithm exhibits high bias and hence high RMSE for the direction estimates. This can be accounted for by the use of only the first order derivative constraint when evaluating the source directions which limits the source bandwidths it can handle. We observe a significant RMSE for the source located at 50° for all SNR conditions due to the reduced degrees of freedom and insufficient derivative constraints.
- At low SNR conditions, the BFW-MUSIC algorithm with $\dim\{\mathbf{E}_s\}=5$ and 6 is observed to perform better than the proposed technique. However, with increasing SNR, the proposed technique displays a better performance than the BFW-MUSIC algorithm for all the signal subspace dimensions.

While the proposed technique yields source estimates with fewer number of snapshots, it is useful to investigate its performance as a function of the number of snapshots that is used to construct the spatial correlation matrix $\mathbf{R}$. For the same experimental setup as the previous experiment, we set the SNR to 5 dB and varied the number of snapshots from 250 to 5000. With a priori knowledge of $\dim\{\mathbf{E}_s\}$ of $\mathbf{R}$, the performance of the BFW-MUSIC algorithm is observed in Fig. 8 to be better than the proposed technique at low SNR values. This improvement is due to the strict derivative constraints of BFW-MUSIC which reduces it to a narrowband problem. However, with increasing number of snapshots, the performance of the proposed technique approaches that of the BFW-MUSIC algorithm. We note that the performance difference is not significant beyond 1500 snapshots which is substantially low when compared to the number of snapshots required for frequency domain techniques.

The capability of the proposed technique to resolute of two closely situated sources is investigated now. Three experiments with two wideband sources of normalized bandwidth equal to 0.23 (and fractional bandwidth of 0.6) were performed. The angular separation between the two sources is 5°, 7° and 9° in each of the experiments, respectively. Fig. 9 shows the resolution capability of the proposed technique when 500 snapshots are used. We observe that the resolution capability increases with increasing SNR. However, the improvement in the probability of resolution with the increase in snapshots is not shown in Fig. 9.

In order to compare the performance of proposed technique with TOPS algorithm, we study the RMSE of the DOA estimates. The number of frequency bins used for DOA estimation with TOPS is equal to the source bandwidth. The frequency-domain snapshots are obtained with a 256-point FFT on the sensor snapshots. While 100 frequency-domain snapshots are used for TOPS algorithm, equivalent number of time-domain snapshots (25 600) is used for the proposed technique. The Cramer–Rao lower

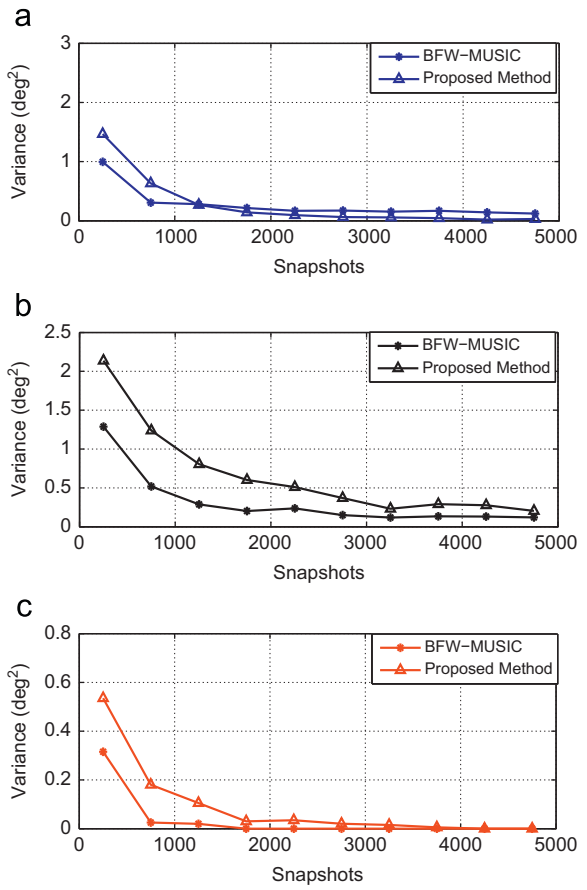

Fig. 8. Variance of the source estimates of BFW-MUSIC algorithm and the proposed technique. (a) Source 1, (b) Source 2 and (c) Source 3.

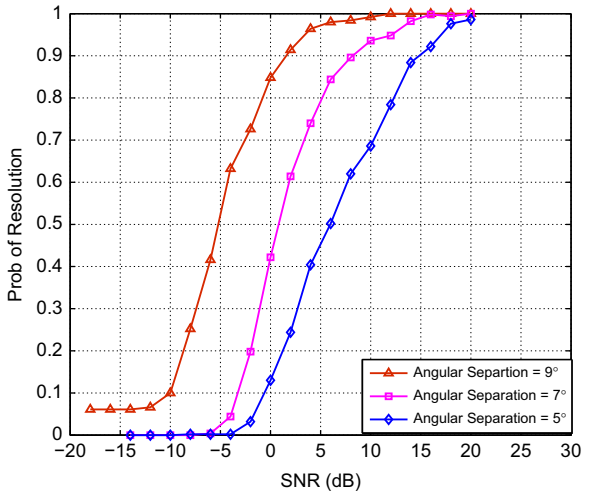

Fig. 9. Probability of resolution for various angular separations of sources. While the first source is situated at 60° for all the three cases, the second source is situated at 65°, 67° and 69° for each case, respectively.

bound (CRLB) for the estimates is evaluated as described in [6] with the knowledge of the signal covariance matrix $\mathbf{R}_{ss}(f)$.

With sampling frequency normalized to unity, all the sources are centered at f_c=0.3 with normalized bandwidths equal to 0.15. Fig. 10 shows the RMSE of the source estimates for all the techniques averaged over 200 iterations along with the CRLB. The proposed technique is observed to have improved performance over TOPS and BFW-MUSIC algorithms. Results shown in Fig. 10 is consistent with the observation made in [12]; the performance of TOPS is comparable with other techniques only at mid and high SNR ranges while a large estimation error is monitored at lower SNR values. In Fig. 8, it was observed that the variance of the estimates from proposed technique approached BFW-MUSIC with an increase in time-domain snapshots. However, at very large number of snapshots, it is evident from Fig. 10 that the performance of BFW-MUSIC remains consistent while the RMSE of the proposed technique continues to decrease, thus achieving better performance over BFW-MUSIC algorithm.

Fig. 11 shows the comparison of the resolution capability of TOPS algorithm, BFW-MUSIC algorithm and the proposed technique. The result corresponds to an angular separation of 6° between the two sources, averaged over 200 trials. It is important to note that the resolution capability of the proposed technique is significantly higher than that of the TOPS algorithm. This improvement

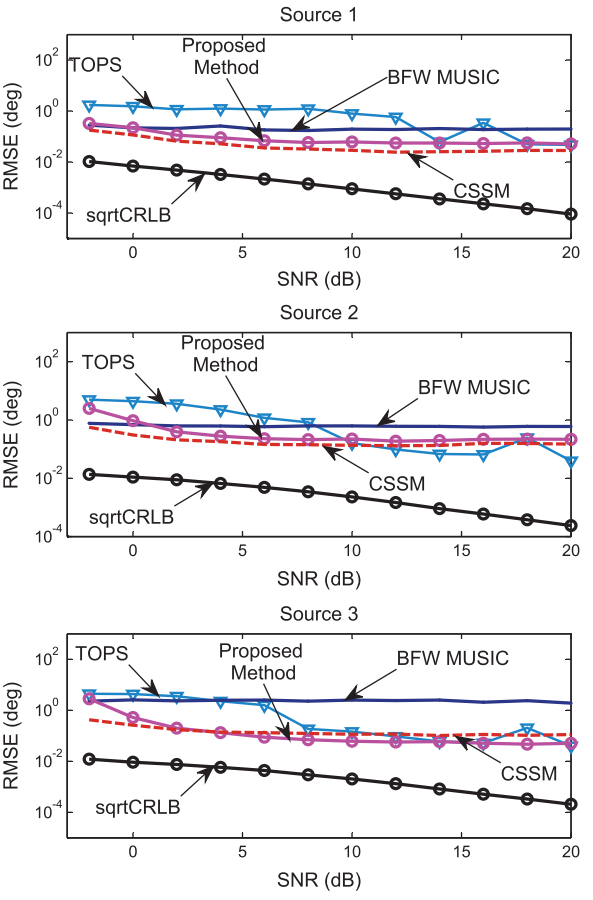

Fig. 10. Estimation performance for TOPS and the proposed method when sources are situated at 70°, 87° and 95°.

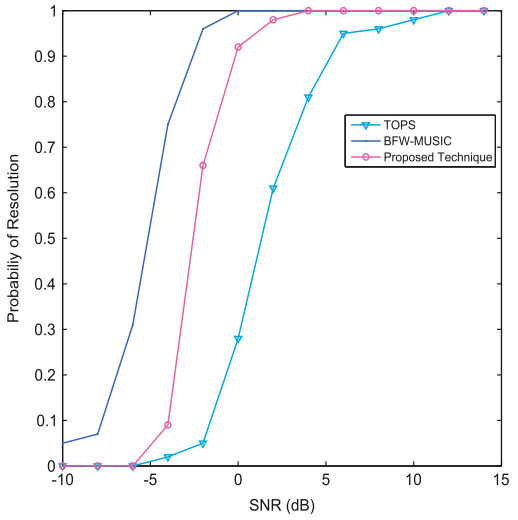

Fig. 11. Comparative study of the probability of resolution between the TOPS algorithm and the proposed method for an angular separation between the sources of 6°. Sources are situated at 40° and 46°.

can be credited to the increased number of time-domain snapshots used in estimating the autocorrelation matrix. However, the resolution capability of BFW-MUSIC algorithm is superior over the proposed technique. With the knowledge of the signal subspace dimension and the imposed linear derivative constraints, BFW-MUSIC can perform better even at lower SNR values. From a comparative study between Figs. 9 and 11, we infer that an increase in the number of snapshots enables the proposed technique to resolve two closely spaced sources at relatively lower SNR values.

5. Conclusion

In this work, a new wideband DOA estimation technique has been proposed which does not require to know the model order. The Taylor series approximation of steering vector w.r.t. frequency enables us to incorporate wideband derivative constraints into the optimization problem. The significant peaks in the spatial spectrum of this beamformer-based estimator are indicative of source directions. The temporal processing of data snapshots has been advantageous in drastically reducing the number of snapshots required for the estimator. The numerical evaluation of the proposed technique validates the advantages of the proposed technique over existing techniques.

Acknowledgments

The authors wish to thank the anonymous reviewers for their valuable comments in improving the quality of this manuscript.

Appendix A. Time-domain wideband covariance matrix

In the time-domain wideband signal model, the array manifold matrix is a continuous function of frequency while the source spectrum need not. Therefore, in the proximity of the reference frequency f_0, $\mathbf{A}(f,\Theta)$ at any frequency f can be expressed using Taylor series expansion up to the Pth order as

$$\mathbf{A}(f,\Theta)\approx\mathbf{A}(f_0,\Theta)+\sum_{p=1}^{P}\frac{\Delta f^p}{p!}\frac{\partial^p}{\partial f^p}\mathbf{A}(f,\Theta)\Big|_{f=f_0}, \tag{30}$$

where

$$\frac{\partial^p}{\partial f^p}\mathbf{A}(f,\Theta)=\left[\frac{\partial^p}{\partial f^p}\mathbf{a}(f,\theta_1)\ldots\frac{\partial^p}{\partial f^p}\mathbf{a}(f,\theta_M)\right]$$

is the pth order derivative array manifold. Substituting (30) in the time-domain signal model (10), we obtain

$$\mathbf{x}(n)=\frac{1}{K}\sum_{k=0}^{K-1}\left\{\mathbf{A}(f_0,\Theta)+\sum_{p=1}^{P}\frac{\Delta f_k^p}{p!}\frac{\partial^p}{\partial f^p}\mathbf{A}(f,\Theta)\Big|_{f=f_0}\right\}\times\mathbf{s}(f_k)e^{j2\pi kn/K}+\mathbf{v}(n), \tag{31}$$

where $\Delta f_k=f_k-f_0$ is the frequency deviation from f_0. Using the relation in (31), the time-domain data covariance matrix can be evaluated as

$$\begin{aligned}\mathbf{R}&=E\{\mathbf{x}(n)\mathbf{x}^H(n)\}\\&=E\left\{\left[\frac{1}{K}\sum_{k=0}^{K-1}\left\{\mathbf{A}(f_0,\Theta)+\sum_{p=1}^{P}\frac{\Delta f_k^p}{p!}\frac{\partial^p}{\partial f^p}\mathbf{A}(f,\Theta)|_{f=f_0}\right\}\mathbf{s}(f_k)e^{j2\pi kn/K}+\mathbf{v}(n)\right]\right.\\&\quad\left.\times\left[\frac{1}{K}\sum_{k=0}^{K-1}\left\{\mathbf{A}(f_0,\Theta)+\sum_{p=1}^{P}\frac{\Delta f_k^p}{p!}\frac{\partial^p}{\partial f^p}\mathbf{A}(f,\Theta)|_{f=f_0}\right\}\mathbf{s}(f_k)e^{j2\pi kn/K}+\mathbf{v}(n)\right]^H\right\}.\end{aligned} \tag{32}$$

Assuming the source spectrum to be uncorrelated across frequency bins, i.e., $E\{\mathbf{s}(f_{k_1})\mathbf{s}^H(f_{k_2})\}=\mathbf{0},\forall k_1\neq k_2$, (32) reduces to (11), with $\mathbf{R}_{ss}(f_k)=E\{\mathbf{s}(f_k)\mathbf{s}^H(f_k)\}$.

References

[1] H.L.V. Trees, Optimum Array Processing, Wiley, 2002.
[2] W.-K. Ma, T.-H. Hsieh, C.-Y. Chi, DOA estimation of quasi-stationary signals with less sensors than sources and unknown spatial noise covariance: a Khatri–Rao subspace approach, IEEE Transactions on Signal Processing 58 (2010) 2168–2180.
[3] P. Pal, P.P. Vaidyanathan, Nested arrays: a novel approach to array processing with enhanced degrees of freedom, IEEE Transactions on Signal Processing 58 (2010) 4167–4181.
[4] M. Wax, T. Shan, T. Kailath, Spatio-temporal spectral analysis by eigenstructure methods, IEEE Transactions on Acoustics, Speech and Signal Processing 32 (4) (1984) 817–827.
[5] H. Wang, M. Kaveh, Coherent signal-subspace processing for the detection and estimation of angles of arrival of multiple wide-band sources, IEEE Transactions on Acoustics, Speech and Signal Processing 33 (4) (1985) 823–831.
[6] B. Friedlander, A. Weiss, Direction finding of wideband signals using an interpolated array, IEEE Transactions on Signal Processing 41 (4) (1993) 1618–1634.
[7] M. Doron, E. Doron, Wavefield modelling and array processing, part II—algorithms, IEEE Transactions on Signal Processing 42 (10) (1994) 2560–2570.
[8] H. Hung, M. Kaveh, Focussing matrices for coherent signal-subspace processing, IEEE Transactions on Acoustics, Speech and Signal Processing 36 (8) (1988) 1272–1281.
[9] M. Doron, A. Weiss, On focusing matrices for wideband array processing, IEEE Transactions on Signal Processing 40 (6) (1992) 1295–1302.
[10] F. Sellone, Robust auto-focusing wideband DOA estimation, Signal Processing 86 (1) (2006) 17–37. doi:10.1016/j.sigpro.2005.04.009.
[11] D.N. Swingler, J. Krolik, Source location bias in the coherently focussed high-resolution broadband beamformer, IEEE Transactions on Acoustics, Speech and Signal Processing 37 (1) (1989) 143–145.

[12] Y.-S. Yoon, L. Kaplan, J. McClellan, TOPS: a new DOA estimator for wideband signals, IEEE Transactions on Signal Processing 54 (6) (2006) 1977–1989.
[13] B.P. Ng, M.H. Er, C. Kot, A MUSIC approach for estimation of directions of arrival of multiple narrowband and broadband sources, Signal Processing 40 (2–3) (1994) 319–323.
[14] M. Wax, T. Kailath, Detection of signals by information theoretic criteria, IEEE Transactions on Acoustics, Speech and Signal Processing 33 (2) (1985) 387–392.
[15] A. Quinlan, F. Boland, J. Barbot, P. Larzabal, Determination of the number of wideband acoustical sources in a reverberant environment, in: Proceedings of the European Signal Processing Conference, 2006.
[16] H. Teutsch, W. Kellermann, Estimation of the number of wideband sources in a acoustic wave field using eigen-beam processing for circular apertures, in: IEEE Workshop on Applications of Signal Processing to Audio and Acoustics, 2005.
[17] P.-J. Chung, J.F. Böhme, C.F. Mecklenbräuker, A.O.I. Hero, Detection of the number of signals using the Benjamini–Hochberg procedure, IEEE Transactions on Signal Processing 55 (6) (2007) 2497–2508.
[18] P.-J. Chung, M. Viberg, C.F. Mecklenbräuker, Broadband ML estimation under model order uncertainty, Signal Processing 90 (5) (2010) 1350–1356.
[19] K.N. Le, A new formula for the angle-of-arrival probability density function in mobile environment, Signal Processing 87 (2007) 1314–1325.
[20] K.N. Le, On angle-of-arrival and time-of-arrival statistics of geometric scattering channels, IEEE Transactions on Vehicular Technology 58 (2009) 4257–4264.
[21] J. Capon, High-resolution frequency-wavenumber spectrum analysis, Proceedings of the IEEE 57 (8) (1969) 1408–1418.
[22] Z. Ying, B.P. Ng, Music-like DOA estimation without estimating the number of sources, IEEE Transactions on Signal Processing 58 (3) (2010) 1668–1676.
[23] K.B. Petersen, M.S. Pedersen, The Matrix Cookbook, October 2008. URL 〈http://www2.imm.dtu.dk/pubdb/p.php?3274〉.
[24] A. Gershman, U. Nickel, J. Bohme, Adaptive beamforming algorithms with robustness against jammer motion, IEEE Transactions on Signal Processing 45 (7) (1997) 1878–1885.
[25] Y.N. Rao, J.C. Principe, An RLS type algorithm for generalized eigendecomposition, in: Proceedings of the 2001 IEEE Signal Processing Society Workshop on Neural Network for Signal Processing XI, 2001, pp. 263–272.